Dynamics of chlorinated aliphatic hydrocarbons in the Chalk aquifer of northern France

Milena Walaszek, Lise Cary, Gabriel Billon, Michaela Blessing, Aurélie Bouvet-Swialkowski, Melinda George, Justine Criquet, Jean Remi Mossmann

Dynamics of chlorinated aliphatic hydrocarbons in the Chalk aquifer of northern France

Walaszek M.[1-2], Cary L.[2*], Billon G.[1], Blessing M.[3], Bouvet-Swialkowski A.[4], George M.[1], Criquet J.[1], Mossmann J.R. [2]

[1] Univ. Lille CNRS, UMR 8516 – LASIRE, Equipe Physico-Chimie de l'Environnement, Lille F-59000, France

[2] BRGM (French Geological Survey), 59810 Lesquin, France

[3] BRGM (French Geological Survey), 45060 Orléans Cedex 2, France

[4] Lille European Metropolis, 59040 Lille Cedex, France

*Corresponding author: Tel.: +33 (0)320191548; E-mail address: l.cary@brgm.fr

1. Introduction

Chlorinated (aliphatic) hydrocarbons (CHCs) such as the common solvents tetrachloroethene (PCE), trichloroethene (TCE) and 1,1,1-trichloroethane (TCA) are among the most common chemicals that pollute groundwaters worldwide (Clement et al., 2000; Witt et al., 2002; Lenczewski et al., 2003; Arianna et al., 2019; Kawabe and Komai, 2019; La Vigna et al., 2019). They are used as industrial solvents for a broad range of applications in chemical synthesis, degreasing agents of metal parts, cleaning of electronic components, or textile dry-cleaning (Rivett et al., 1990), and are known or suspected to be carcinogenic or mutagenic agents for humans. Natural CHC attenuation occurs under both reducing and oxidizing conditions in groundwater, mainly leading to the formation of less chlorinated compounds such as *cis*-1,2-DCE, 1,1-DCE, 1,2-DCE and 1,1-DCA. Depending on the physico-chemical conditions, these intermediate products can be further degraded to vinyl chloride (VC), ethene and ethane.

During reductive dechlorination, chlorine atoms are sequentially removed and replaced with hydrogen; the transformation proceeds from PCE to TCE, to *cis*-dichloroethene (*cis*-1,2-DCE), to vinyl

chloride (VC), and from 1,1,1-TCA to 1,1-DCA to chloroethane (CA), and finally to non-toxic ethene/ethane (Vogel et al. 1987, Wiedemeier et al. 1999). Under anaerobic conditions, 1,1,1-TCA may also be degraded abiotically by α-dehaloelimination to 1,1-DCE (Vogel and McCarty, 1987). Commonly, 1,2-DCE and 1,1-DCA accumulate due to incomplete reduction; high concentrations of co-contaminants can also inhibit dechlorinating bacteria (Maymó-Gatell et al., 2001; Kawabe and Komai, 2019). Under oxic conditions, DCE, VC and TCE can be directly mineralized to CO_2 via oxidative pathways (Clement et al. 2000). As dense compounds, CHCs have a tendency for downward migration, transport along fractures, and settling in pools at the base of the aquifer. Less chlorinated daughter products are more mobile in groundwater than PCE or TCE. It has been observed that each of these dechlorination steps is leading to a significant carbon isotope fractionation within the molecules that are involved in the degradation reactions (Hunkeler et al., 1999; Bloom et al., 2000; Sherwood Lollar et al., 2001). Compound- and pathway-specific fractionation factors α (which define the isotopic fractionation between any two compounds) or the enrichment factor ε are determined in laboratory batch or column systems with pure or mixed microbial cultures by applying the Rayleigh equation (Braeckevelt et al., 2012).

Numerous studies have explored CHC spatial dynamics, mainly focusing on the remediation of contaminated sites with often identified and finite-source pollutions (Clement et al., 2000; Witt et al., 2002; Pooley et al., 2009; Palau et al., 2014; Wanner and Hunkeler, 2015; Arianna et al., 2019). Most studies used classic sampling methods based on pumping at one depth. However, such sampling may be inadequate for characterizing the potential stratification of such pollution. For this purpose, passive diffusion samplers were developed for monitoring CHCs in groundwater (Vroblesky and Campbell, 2001; Divine et al., 2004; Divine and McCray 2004). Such samplers consist of a sealed semipermeable membrane (such as low-density polyethylene (LDPE)) full of pure water, whose concentration increases until equilibrium with the ambient concentrations is reached.

In the peri-urban area of southwest Lille (Figure 1), with its mixed agricultural and industrial activities, the Chalk aquifer used for drinking-water production is threatened by the presence of CHCs. Droughts are more frequent and severe in the region since a few years, and the groundwater level has been lowering since 2017. Therefore, the decrease of water *quantity* in the aquifer and the continuing pumping operations cause a decrease in water *quality*. CHC concentrations in groundwater commonly exceed the European water guideline for drinking water ([PCE] + [TCE] <10 µg L^{-1}, (RF, 2007)) thus limiting the use of this resource for drinking-water production (40% of the needs of the 1 million inhabitants of the Lille European Metropolis). A good understanding of CHC dynamics and their spatial distribution in the aquifer thus is a key factor, especially in the case of VC, the most toxic and carcinogenic CHC (Lee et al., 1977; Clewell et al., 1995; Giri, 1995) with the most drastic restrictive regulation [VC <0.5 µg L^{-1}, (RF, 2007)].

To our knowledge, no studies have determined the CHC degradation processes in groundwater over time, and in a large number of multiple well fields. In this paper, sharp investigations of the dynamics and degradation processes of CHCs were performed over a large complex area (2,032 ha) in terms of hydrology, geology and contamination sources at the catchment scale composed of several well fields. Wells were sampled during eight years to evaluate CHC concentrations, using standard one-depth sampling. To assess a possible migration or degradation of the compounds, intensive sampling of some wells along the water column with passive samplers were undertaken as well as compound-specific carbon-isotope analyses. Finally, a detailed hydrochemical definition of the area allows strengthening our conclusions.

2. Material and methods

2.1. Geological and hydrogeological context

In the study area, the stratigraphic succession of the Paris Basin begins with a highly faulted, more-or-less dolomitic, several-hundred-meters-thick succession of Lower Carboniferous limestone and calcareous shale (Cary et al., 2014). This is overlain by marly Cenomanian Chalk, locally called the ‘‘Dièves’’, resulting from the Cretaceous transgression. The ‘‘Dièves’’ is followed by a thick deposit of Turonian marly limestone that evolves upward to white and grey flint-bearing Turonian and Senonian Chalk with phosphate beds. The unconformably overlying Tertiary formations comprise the Louvil Clay (Lower Landenian, 9–12 m thick), the Ostricourt Sand (Upper Landenian, 25–30 m thick), and the Flandres Clay (Ypresian, 10–15 m thick). Throughout the Paris-London Basin, the Tertiary formations confine the underlying Chalk aquifer. Quaternary loess (pre-Weichselian and Weichselian) covers practically the entire basin. The uppermost 5 m in the Lille region consist of Quaternary alluvium of the Deûle canal, mainly comprising heterogeneous sandy/clayey deposits.

The Dièves marl is the impermeable base of the Chalk aquifer. This is constituted by the Turonian-Senonian Chalk at 10–50 m depth, favoured by the presence of highly permeable horizons with open fissures mainly found at 10–15 m depth. The groundwater of the Chalk aquifer circulates in the fault network, which is highly developed in the valleys where the well fields are sited (Cary et al., 2014).

Drinking water for the Lille European Metropolis is pumped from four well fields tapping the Chalk aquifer to the southwest of Lille, the Emmerin (5,346 ha), Houplin-Ancoisne (6,303 ha), Les Ansereuilles (8,298 ha) and Seclin (369 ha) well fields (Figure 1). The Emmerin well field (10 pumping wells) is located at the top of a WNW-ESE anticline. The Houplin-Ancoisne well field (11 pumping wells) lies along the Seclin canal that follows the trajectory of the major NW–SE-trending Seclin Fault; here the Chalk groundwater is locally confined below clayey deposits. The Les Ansereuilles well field (26 pumping wells) is parallel to the highly polluted Deûle canal. The groundwater, which is

unconfined southwest of the Deûle, flows northwest to become confined under the alluvial cover that can be 15–20 m thick. In the A12–A15 well area it is locally confined due to the presence of more than 10 m of clay deposited above the Chalk (Cary et al., 2014). The Deûle canal and other small tributaries drain the area, which is affected by quantitative and qualitative pressures of industrial, urban and agricultural origins.

Inverse modelling with the MARTHE software has used potentiometric data from the studied well fields (Bessière et al., 2015). The simulation results show the reversed water pathways from selected starting points (pumping wells) to the probable origin (blue lines on Figure 1). Groundwater-drawdown areas are centred around the groups of exploited wells. For example, four groundwater drawdowns are identified in the Les Ansereuilles well field: the northern part centred around A16, the northwestern part around A26, the southwestern part around A18, and the southern part around A21.

In all, 363 current and former industrial sites potentially involved in or identified as responsible for CHC pollution are stored in the BASIAS database (https://www.georisques.gouv.fr/dossiers/basias/) of French well fields. More than 20% of these sites are metalworking plants (boiler work, automobile factory, sheet-metal manufacture, foundry, etc.) that use PCE, DCE and TCA for metal cleaning. Industrial laundries, chemical plants, and textile and dyeing factories using these CHCs were also identified in the well fields (Figure 1). The difficulties of waste management and recycling in the past caused the storage of CHCs close to groundwater.

Figure 1: Location of the 22 studied wells, geological formations, modelled water pathways and (suspected) industrial sources of chlorinated solvents in the four studied well fields (shown by ellipses).

2.2. Sampling and analyses

Groundwater was sampled by quarterly pumping in 22 wells from 2011 to 2019, to evaluate the chlorinated-solvent concentrations at one depth. Twelve wells were located in Les Ansereuilles (A12, A13, A14, A15, A16, A18, A21, A26, PZ49, PZ55, PZ56, and PZ59), five in Houplin-Ancoisne (H1, H4,

H7, H11, and PZ51), four in Emmerin (E5, E7, E8, and PZ61) and one in Seclin (S1) well fields (Figure 1).

Among the large panel of studied wells, a more detailed analysis has been performed on three wells (PZ56, PZ59, and PZ61) located in three strategic locations of the well fields (northern and southern parts of Les Ansereuilles, Emmerin, respectively). These wells were sampled along the water column with passive samplers (low density polyethylene diffusion bags filled with ultrapure water: 100 µm thick, 90 cm high, 4 cm large, volume 300 mL), to assess a possible vertical migration of the compounds during a further ten sampling campaigns from 2016 to 2019 during different seasons. The well cross-sections are shown in the Supplementary Information (Fig. SI-1). Deployment of the passive samplers depended on the inflows measured along the water column (PZ56: 6 inflows, 8 sampling depths from -19.5 to -52.6 m; PZ59: 3 inflows, 10 sampling depths from -7 to -64.3 m; PZ61: 5 inflows, 5 sampling depths from -9 to -23.2 m). Inflows were obtained along vertical profiles using flowmeter measurements (GFTC probe, SEMM logging, France) from the piezometric level to the bottom of the well. Velocity measurements were taken every 0.5 m (Maréchal et al., 2004). During pumped and passive samplings, samples were collected in filled to capacity brown glass bottles, stored in a refrigerated cooler and carried to the laboratory where CHC analyses were made within 24 h. The presence of CHC-degradation marker gases (CO_2, methane, ethane, ethene) was investigated in November 2017. Compound-specific carbon-isotope analysis was used to gain further insight into the intrinsic biodegradation of chlorinated solvents within the aquifer. To this end, three campaigns in 2017, 2019 and 2020 pumped samples from the six observation wells (Fig. 1); some samples were taken at two depths. In addition, a more detailed *in-situ* hydrochemical definition of groundwater studied physico-chemical parameters. Redox potential Eh (whose values are expressed against the SHE electrode) and dissolved oxygen were recorded with a multiparameter probe (EXO 1, YSI Incorporated, Yellow Springs, Ohio, USA).

The CHC concentrations in sampled groundwater (PCE, TCE, TCA, *cis*-1,2-DCE, *trans*-1,2,DCE, 1,1-DCE, 1,2-DCE, 1,1-DCA, 1,2-DCA and VC) were measured using a HS-GC-MS-MS (Thermoelectron Triplus Duo-Trace GC Ultra-TSQ Quantum XLS) with a quantification limit of 0.2 µg L^{-1} and an accuracy of 5 to 10% depending upon the concentration. Analyses were performed by the Lille European Metropolis laboratory within one day after sampling the groundwater.

Gases were analysed by the BRGM laboratory using a Trace GC Ultra Thermo Fisher Scientific gas chromatograph (Thermo Scientific, with FID detector). The gases investigated were CO_2 and C_nH2_{n+2} (n=1 to 2) with injection valves of 25 µL and 250 µL). Detection limits were ±0.0002% for C_nH_{2n+2} and ±0.001% for CO_2. Percentages are volumic.

Compound specific isotope analysis (CSIA) is an analytical method that measures the ratio of stable isotopes of a contaminant. Stable carbon-isotope ratios of individual CHC compounds were determined by gas chromatography - combustion – isotope-ratio mass spectrometry (GC-C-IRMS) using a Trace GC Ultra gas chromatograph (Thermo Scientific) equipped with a Rtx-VMS column (60 m x 0.32 mm, 1.8 µm film) connected via a GC IsoLink combustion interface to a Delta V Plus isotope-ratio mass spectrometer (Thermo Scientific). The system was used together with a Combi Pal autosampler where headspace extraction of the water samples was performed by in-tube microextraction (ITEX-2) using a Tenax GR with 80/100 mesh size as sorbent material (ITEX-trap from BGB Analytics); see (Laaks et al., 2010) for further details. Isotopic ratios of each compound are expressed in ‰ difference relative to the VPDB (Vienna Pee Dee Belemnite) international standard using the delta notation given by: $\delta^{13}C = (R/R_{std} -1)*1000$, where R and R_{std} are the isotope ratios of the sample and the VPDB standard, respectively. Analytical uncertainty (including reproducibility and accuracy) for the given compounds is generally within ±0.5‰. Isotopic measurements were performed in triplicate. The method quantification limit was equal to 5 µg L^{-1} for TCE and PCE, 15 µg L^{-1} for *cis*-1,2-DCE and 20 µg L^{-1} for all other CHCs. Isotope fractionation can be expressed by

enrichment factors $\varepsilon = \delta^{13}C_o - \delta^{13}C_p$, where $\delta^{13}C_p$ is the carbon isotope ratio of the product and $\delta^{13}C_o$ the carbon isotope ratio of the corresponding precursor (Hunkeler et al., 1999).

3. Results

The mean concentrations and standard deviations of CHCs from standard sampling (2011 to 2019 data) are provided in the Supporting information in Table SI-1. The CHC concentrations from passive sampling in the wells at each depth (2016-2018 data) are presented in the Supporting information in Table SI-3 and summarized with mean-values by depth in Table SI-2.

3.1. CHC pollution in the well fields

Groundwater in the southwest of the Ansereuilles well field showed the highest average CHC concentrations (PZ59: 185 µg L^{-1}, PZ56: 150 µg L^{-1}, A18: 65 µg L^{-1}, Figure 2-a). To a lesser extent, CHCs were detected in PZ55 and A21 (respectively 30 and 9 µg L^{-1}). Downstream of the Deûle canal, CHC concentrations decreased from 25 µg L^{-1} (A12) to 1.4 µg L^{-1} (A14). The Houplin-Ancoisne and Emmerin well fields were less affected by CHC pollution (H7: 9 µg L^{-1}, E7: 2 µg L^{-1}, and PZ61: 14 µg L^{-1}). No CHCs were detected in A26 and H11. In addition, the distribution of the various CHC compounds differed from one well to the next (Figure 2-b). In the southern part of the Ansereuilles well field, either *cis*-1,2-DCE or PCE represented more than 60% of the total concentration (PZ59, A18 and PZ49: *cis*-1,2-DCE, A21 and PZ55: PCE). In such highly polluted wells and at these single-depth sampling points, the degradation products were often not detected. However, in the northern half of the Les Ansereuilles almost all CHC compounds were detected, the major compound representing <40% of the total mass concentration. In the Houplin-Ancoisne and Emmerin well fields PCE dominated, followed by TCE and 1,1,1-TCA., except in E8 where TCA was the major compound. In Seclin, TCE was the only compound detected.

Figure 2: (a) Average total CHC concentrations in µg L^{-1} in the studied well fields (data from 2011 to 2019). Colours of symbols are shaded according to the CHC concentrations. (b) CHC distribution in percentage (%), each colour represents a CHC compound (H11 and A26 not shown because of the absence of CHCs).

3.2. CHC concentrations along depth and over time

Pearson coefficients were computed to investigate possible correlation between piezometric levels and CHC concentrations at multiple depths between 2016 and 2019. Pearson coefficients are significant if $R_{critical} > 0.7$ (with p-value=0.05). Results are presented in Table SI-4. In PZ61, pearson coefficients are positive and from 0.73 to 0.97 at -9 m for 1,1-DCE, 1,1,1-TCA, TCE and PCE. For PCE, pearson coefficients are superior to 0.7 and significant at -13 and -19.45m, too. In PZ56, pearson coefficients are positive from 0.72 to 0.99 at -19.5, -25, -31 and -41m for 1,1-DCA, *trans*-1,2-DCE and PCE. At -52.6 m, pearson coefficients are negative from -0.82 to -0.70 for 1,1-DCE, 1,1-DCA, *cis*-1,2-DCE, 1,1,1-TCA, TCE and PCE. In PZ59, peason coefficient is positive (0.95) for *cis*-1,2-DCE at -10 m and negative (-0.71) for *trans*-1,2-DCE at -53 m. In PZ61 at -15.75m, high concentration of PCE is observed during the high water-level period (14.0 µg L^{-1} in February 2018) while low concentration of PCE is observed during the low water-level period (8.3 µg L^{-1} in September 2018).

CHC concentrations in PZ56, PZ59 and PZ61 were sampled with PDB along the water column over ten sampling campaigns from 2016 to 2019. All results are shown in Supporting Information (Table SI-3). In PZ56, all CHC compounds were detected in the water column (from -19.5 to -59 m), except 1,2-DCA that was below the quantification limit (0.2 µg L^{-1}). VC was detected at the deepest point of the water column (-59 m, 0.2 µg L^{-1}). TCE, PCE, *cis*-1,2-DCE, 1,1-DCA and 1,1,1-TCA concentrations decreased with well depth. In PZ59, no CHCs occurred in the first metres of the water column, but were observed from -33.6 to -64.3 m, especially *cis*-1,2-DCE whose concentration decreased with depth (from 160 µg L^{-1} at -47 m to 70 µg L^{-1} at -64.3 m),. 1,1-DCE and VC were detected, but at low concentrations (respectively ≤0.3 µg L^{-1} and from 0.2 to 1.1 µg L^{-1}). Chlorinated ethanes were not detected, except minor 1,1-DCA with concentrations <2.9 µg.L^{-1}. In PZ61, only PCE, TCE and TCA were

detected along the water column (from -9 to -23.2 m) with a peak at -13 m and a subsequent decrease with depth (PCE: 10.1 to 3.0 µg L^{-1}, TCE: 1.2 to 0.5 µg L^{-1}, TCA: 0.8 to 0.3 µg L^{-1}).

Figure 3 shows the evolution of total CHC and of two predominant CHC compounds concentrations over time at multiple depths sampled in PZ56, PZ59 and PZ61. All depths were not sampled for each campaign, the absence of data at some depths in 2016 and 2019 does not mean that the CHCs were under the limit of detection but were not investigated. In PZ56, CHCs were detected from -19.5 m to the bottom (-59 m) and decreased along depth: the average total CHCs concentrations varied from 147 µg L^{-1} at -19.5 m to 42 µg L^{-1} at -59 m. In the first part of the well (from -19.5 m to -47m), CHC concentrations increased over time (at -19.5m, from 86 µg L^{-1} in 2017 to 188 µg L^{-1} in 2019) while they were quite stable at the bottom of the well (at -59 m, 51 µg L^{-1} in 2016 to 36 µg L^{-1} in 2018). The piezometric level decreased from -14.03 m in August 2016 to -15.88 m in October 2019, with a peak at -13.70 in June 2018. In PZ59, CHCs were detected from -26 m to the bottom (-64.3 m) and concentrations increased from 0.2 µg L^{-1} at -26.7 m to 180 µg L^{-1} –at 67.3 m. The piezometric level decreased from -2.7 m in August 2016 to -5.26 m in October 2019 with a rise at -3.8 in February 2018. In PZ61, CHCs were detected from -9 m to -23.2 m. In the first meters of the water column (-9 to -15.75 m), CHCs concentrations increased with depth, besides in September 2018 where concentrations decreased along the entire water column. Then from -15.75 m to the bottom of the well, CHCs concentrations decreased along depth from 12.5 µg L^{-1} at--15.75 m to 3.9 µg L^{-1} at -23.2 m. The piezometric level decreased from -5 m in August 2016 to -7.7 m in October 2019, with a rise at -5.4 m in February 2018.

Figure 3 : Sum of CHCs and predominant CHC compounds concentrations along the water column and variations of the piezometric level over time (2016-2019) for the wells PZ56, PZ59 and PZ61

3.3. Physico-chemical conditions in the wells

Carbon dioxide, methane, ethane and ethene gases were analysed as they provide insight into the final degradation products of CHCs. In PZ56 and PZ61, only CO_2 was detected at 1900 µmol.L^{-1} (-

19.5 m) and 2000 µmol.L^{-1} (-15 m), respectively. In PZ59, at -40 m, CO_2, methane and ethane were found with 2700, 2.9 and 0.09 µmol.L^{-1} at -40 m and 2100, 2.1 and 0.04 µmol.L^{-1}. at -60 m, respectively.

The major inflows and redox potential (Eh) were recorded and analysed along the depth of the three wells. The physico-chemical parameters were recorded during three campaigns (February 2017, November 2017 and February 2018). Only November 2017 data are shown on **Figure 4**, as there were no significant changes between the three campaigns. In PZ56, redox potential increased from 223 mV -20 m to 237 mV at the bottom of the well. In PZ59, redox potential values decreased quickly with increasing depth from 201 mV at -7 m to 84 mV at -30 m and then decreased until 69 mV at the bottom of the well. In PZ61, redox potential values first slightly increased from 241 mV at -10 m to 262 mV at -19 m and then decreased until 122 mV at the bottom of the well.

Figure 4: Depth-specific in-situ groundwater physico-chemistry in observation wells PZ56, PZ59 and PZ61. Redox potential are presented for November 2017.

3.4. Compound-specific isotope compositions

Stable carbon-isotope ratios ($\delta^{13}C$) of CHC compounds were analysed in wells PZ49, PZ55, PZ56, PZ59 and PZ61 in 2017, 2019 and 2020, and in A18 in 2020. The method relies on differences in reaction rates between molecules with light and heavy isotopes during transformation reactions, which causes an enrichment of heavy isotopes (^{13}C) in the residual contaminant fraction. Results are presented in Table 1. Considering the range of analytical uncertainties for these compounds (±0.5‰), most wells showed no variation in $\delta^{13}C$-values throughout the duration of the monitoring survey.

In PZ49, only *cis*-1,2-DCE was detected with constant $\delta^{13}C$ values ranging within analytical uncertainty (≤ ±0.5‰) from -29.8 to -29.6 ‰, between 2017 and 2020. Cis-1,2-DCE concentrations fluctuates from 18.5 to 42 µg L^{-1} in 4 years. In PZ56, CHCs and their potential daughter products were detected at the two sampled depths (-19.5 and -47 m). In 2019 at 19.5 m, higher concentrations accompanied

more depleted $\delta^{13}C$ values of PCE, TCE, *cis*-1,2-DCE, 1,1,1-TCA and 1,1-DCE compared to 2017. In 2019, relatively homogeneous concentrations along the water column (from -19.5 to –47 m) were observed together with constant carbon-isotope ratios over depth. At -19.5 m, $\delta^{13}C$ values of PCE, TCE, *cis*-1,2-DCE, 1,1,1-TCA and 1,1-DCA decreased between 2017 and 2019 (respectively -0.1, -2.1, -0.3, -1.1, -0.5‰) (no analysis at -47 m in 2017). 1,1-DCE was not detected at -19.5 m in 2017. In 2020, TCE and PCE were detected at -19.5 m and only TCE at –47 m, with enriched $\delta^{13}C$ values compared to 2017 and 2019.

In PZ59, only TCE and *cis*-1,2-DCE were detected at -40, -47 and -60 m. For TCE, the $\delta^{13}C$ was constant between 2017 and 2019 along the water column at around -24‰ (Table 1). Then, $\delta^{13}C$ values increased for TCE at -40 m (+1.8‰ between 2019 and 2020) and at -60 m (+0.9‰ between 2017 and 2020). For *cis*-1,2-DCE, $\delta^{13}C$ values were constant between 2017 and 2020 at -40, -47 and -60 m. Only PCE was detected with an enriched $\delta^{13}C$ value (+2.2‰), accompanied by a strong concentration decrease in PZ55 and a constant value -23.3‰ (±0.1‰) in PZ61 between 2017 and 2019. In 2020, CHC concentrations detected in A18 (*cis*-1,2-DCE at 3.6 µg L^{-1}, and TCE at 0.92 µg L^{-1}) were below the quantification limit for isotopic analysis.

Table 1: Stable carbon-isotope ratio $\delta^{13}C$ (in ‰ *vs* VPDB, ±0.5‰) and concentrations (µg L^{-1}) in the wells PZ49, PZ55, PZ56, PZ59 and PZ61 at several depths in 2017, 2019 and 2020.

4. Discussion

4.1. Les Ansereuilles well field

The CHC distribution in the Ansereuilles well field occurred as three separate sectors according to the drawdown areas (Figure 1). The southwestern drawdown, centred around well A18, presented the highest CHC concentrations, from 55.7 µg L^{-1} (PZ49) to 185.2 µg L^{-1} (PZ59), consisting of mostly *cis*-1,2,-DCE and a small amount of TCE. As showed on Figure 2-a, wells PZ59 and A18 pump groundwater from an industrial area. Two former industrial laundries were located upstream of the

287 wells (red targets on Figure 2-a). The Lille European Metropolis has identified one of these laundries
288 as a high CHC-polluted site. TCE and *cis*-1,2-DCE were found in the soil of this site (0.2 m deep, TCE:
289 93 µg g^{-1}, *cis*-1,2-DCE: 2.9 µg g^{-1}) and high CHC concentrations occur in the directly underlying
290 groundwater (*cis*-1,2-DCE: 430 µg L^{-1}, TCE: 43 µg L^{-1}; (Arcadis, 2016)). In PZ59, the $\delta^{13}C$ values of *cis*-
291 1,2-DCE (-31.9 to -31.6‰) were depleted compared to TCE (-24.3 to -22.4‰). This isotopic pattern is
292 consistent with isotope enrichment ε_{TCE} factors being between -18.8 and -6.6‰ (-9.5 to -7.8‰ in
293 PZ59) for reductive dechlorination of TCE (Bloom et al., 2000; Sherwood Lollar et al., 2001; Slater et
294 al., 2001; Aeppli et al., 2009). This may indicate that *cis*-1,2-DCE is a degradation product of TCE
295 (Table 1). In PZ59 (Figure 3), CHCs were found along the water column below -26 m with increasing
296 concentrations for all compounds, suggesting CHC migration without degradation along the well.
297 However VC was found at low concentrations (<1.2 µg L^{-1}) and persistent along the water column
298 (Table SI-3). In addition, methane and ethane occurred at -40 and -60 m. The presence of VC, ethane
299 and methane, and the favourable physico-conditions in the well (reducing conditions, Eh <80 mV,
300 Figure 4) suggest reductive dechlorination of a small amount of *cis*-1,2-DCE until methane. But the
301 highly depleted isotopic signatures of *cis*-1,2-DCE from -31.9 to -31.6‰ also indicate that this
302 compound is accumulating and further degradation to VC concerned only a small amount of *cis*-1,2-
303 DCE (Table 2). Furthermore, for TCE, decreasing concentrations at -40 m between 2017 and 2020 (22
304 to 8.6 µg L^{-1}) and the enrichment of isotopic values in 2020 compared to 2019 (-24.2 to -22.4‰,
305 Table 1) could be the beginning of an active biodegradation as a result of the excavation work of
306 2019 at the polluted site farther upstream (40,000 tonnes of polluted soil excavated). The slightly
307 enriched (compared to PZ59) and steady isotopic signatures of *cis*-1,2-DCE in PZ49 since 2017 suggest
308 the same degradation process in this well as in PZ59 located further upstream. In the well A18
309 located downstream, only very small amounts of CHC have been detected in 2020, compared to
310 relatively high concentrations last measured in 2017, suggesting that the degradation of CHCs is
311 actively ongoing and almost complete within the well. Due to the successful upstream remediation of
312 the source, no further CHCs should be reaching this well.

313 The southern drawdown around well A21 was characterized by major PCE contents (29 µg L^{-1} in PZ55
314 and 8.8 µg L^{-1} in A21). Both wells are also located downstream of several industrial laundries, textile
315 factories and dyeing industries (red and blue targets, Figure 2-a). While no PCE-degradation products
316 were found in PZ55, TCE and DCE were detected at low concentrations in A21 (respectively 0.6 and
317 0.12 µg L^{-1}). The decreasing concentrations of PCE (29 to 5.1 µg L^{-1}, Table 1) and the enriched $\delta^{13}C$
318 values (-28.1 to -25.9‰, Table 1) between 2017 and 2020 in PZ55 indicated biodegradation under
319 reducing conditions in this well, resulting in the DCE found in downstream well A21 (Table 1). The
320 assumption of biodegradation reactions is only valid if the two groundwater layers where sampling
321 took place are directly connected. Another hypothesis for the differences in values observed in well
322 Pz55 for the two different depth intervals that are 14 m apart, might be that there are two different
323 sources of PCE contamination.

324 Finally, the northern drawdown around well A16 was characterized by a mix of different CHC
325 compounds at concentrations ranging from 24.5 µg L^{-1} (A12) to 1.4 µg L^{-1} (A14), including primary
326 products (PCE, TCE, 1,1,1-TCA) and all potential degradation products in variable proportions (*cis*-1,2-
327 DCE, *trans*-1,2-DCE, 1,1-DCE, 1,2-DCE, 1,1-DCA and VC). Well PZ56 was an exception here because of
328 its high CHC concentration (150 µg L^{-1}). A former industrial laundry site, potentially the source of this
329 CHC pollution, lies upstream from the well (red target, Figure 2-a). In PZ56 (Figure 3), CHC
330 concentrations decreased along the water column below -19.5 m with, suggesting migration and
331 dilution of the CHCs in the well. VC was mostly below the quantification limit (0.2 µg L^{-1}) in the water
332 column (Table SI-3). The isotopic signatures of *cis*-1,2-DCE (-23.2 to -22.9‰, Table 1) compared to
333 TCE (-22.6 to -17.7‰) also indicate that *cis*-1,2-DCE may be a degradation product of TCE in PZ56.
334 However, the depleted isotopic signatures of PCE (-24.9 to -23.9‰) compared to *cis*-1,2-DCE and TCE
335 either suggest that these compounds are not degradation products of PCE, or that the dechlorination
336 reaction of TCE and *cis*-1,2-DCE is ongoing and isotopic enrichment even exceeds the isotopic
337 signature of PCE. This latter hypothesis is supported by Rayleigh enrichment factors for reductive
338 dehalogenation that are smaller for PCE (εPCE -3.6 to -5.6‰; (Slater et al., 2001; Wiegert et al., 2013;

339 Badin et al., 2014)), and increase for each of the consecutive metabolites (-13.8, -20.4, -22.4 for TCE,
340 *cis*-1,2-DCE and VC, respectively, (Slater et al., 2001)). The depleted isotopic values of 1,1-DCA (-22.1
341 to -21.6‰, Table 1) compared to TCA (-20.2 and -21.3‰ at -19.5 m) indicate that 1,1-DCA is a
342 possible degradation product of TCA. However, no further interpretations are possible, as reported
343 enrichment factors for biodegradation of 1,1,1-TCA to 1,1-DCA can be small (-1.8‰, (Sherwood Lollar
344 et al., 2001)) or quite large (up to -14‰, (Broholm et al., 2014)). Considering the other compounds,
345 an inversion of the TCA isotopic signature at -47 m is noticed (TCA -23‰ at -47 m and enriched to -
346 21.3‰ at -19.5 m in 2019), compared to TCE that has an opposite behaviour (highest value at -47 m,
347 -20.5‰, and depleted at -19.5 m, -22.6‰, in 2019). This inversion suggests potentially different TCA
348 sources at these two depths. A surprising result is the isotopic signature of 1,1-DCE (-18.7 and -
349 17.5‰). These heavy $\delta^{13}C$ values, compared with the potential primary CHC products (*cis*-1,2-DCE:
350 from 23.2 to 22.9‰, TCE: from -22.6 to -20.5‰, TCA: from -21.3 to -20.2‰), do not allow concluding
351 about a formation of 1,1-DCE by TCE anaerobic biodegradation, nor about an abiotically produced
352 metabolite of 1,1,1-TCA by dehydrochlorination. In addition, the presence of 1,1-DCE as a primary
353 product cannot be excluded due to its use in the plastics industry. In general, the isotopic signature
354 of manufactured solvents is more depleted (<-20‰) (Slater et al., 2001) and the observed $\delta^{13}C$ value
355 of 1,1-DCE might also be an indicator for ongoing *in-situ* biodegradation in this well. In a study by
356 Hunkeler et al. (2002), 1,1-DCE transformation was very fast compared to other compounds. Isotope-
357 enrichment factors for biodegradation of this compound are between -5.8‰ and -7.3‰ (Hunkeler et
358 al., 2002; Lee et al., 2007), supporting the idea of 1,1-DCE biodegradation in this well. However, as
359 the initial source values are unknown, this shows that the isotope approach has its limitations for an
360 intermediate compound that is simultaneously formed and degraded. With the limited number of
361 monitoring wells and data currently available, we cannot conclude whether TCE was added from
362 additional sources or derives from the dehalogenation of PCE. 1,1-DCE, too, may have been added
363 from another source, or may stem from the dehydrochlorination of 1,1,1-TCA (Table 1).

In the Ansereuilles well field, in addition of the importance of the pollution sources, the geology further influences the CHC concentrations in groundwater. The clay deposits at the top of the northern wells (A13 to A15) confine the groundwater, causing reducing conditions. As shown on Figure 5, the wells under reducing conditions (redox potentials from 163 mV in A15 to 236 mV in A13, according to Sigg (2000)) had the lowest CHC concentrations (from 1.4 in A14 to 12.3 µg L^{-1} in A13) with low detection frequency. These low CHC concentrations are consistent with low nitrate concentrations (from below the detection limit in A14 to 8.6 mg L^{-1}) which are an evidence of denitrification processes occurring under reducing conditions, while the wells are located in an agricultural area where high nitrate concentrations can be found in the groundwater under oxidizing conditions (for example, 20-40 mg L^{-1} in A18, Figure 5). On the contrary, the wells under oxidizing conditions (A10, A11, A18 and PZ56, redox potentials from 315 mV in A18 to 436 mV in PZ56) had the highest CHC concentrations with high detection frequency and high nitrate concentrations. The well A12 is located in a transition zone and present moderately reducing condition (redox potential: 300 mV), low CHC concentrations with high detection frequency and high nitrate concentrations. Finally, the well PZ59 that is near a major source of TCE presents high CHC concentrations under reducing conditions along with low nitrate concentration.

Figure 5: Redox potential (mV), nitrates (mg L^{-1}) and total CHC concentration (µg L^{-1}) according to location (Lambert 93 X coordinate) in the Ansereuilles well field

4.2. Emmerin, Houplin-Ancoisne and Seclin well fields

The Emmerin well field was separated into two different areas. The first one contains wells E7, E5 and PZ61, with low CHC concentrations ranging from 1.7 µg L^{-1} (E7) to 15.8 µg L^{-1} (PZ61). PCE was the most common pollutant in the wells, with lesser amounts of TCA and 1,1-DCE. The second area is around the far western well E8, where TCA dominates followed by TCE, PCE and their degradation products as *cis*-1,2-DCE, 11-DCE and 1,1-DCA. In PZ61, CHC concentrations decreased downward (data in Supporting Information, Table SI-3). The steady isotopic signature of PCE between 2017 and

2020 (-23.3 and -23.4‰) suggested that this compound was not further degraded in the well. The isotopic signature of PCE in PZ61 can be compared to initial pure phase $\delta^{13}C$ values of PCE ranging from -37.2 to -23.3‰ (van Warmerdam et al., 1995). Being at the upper end of reported values either Pz61 represents source values that have never been subject to biodegradation, or as we don't know the initial source of this contamination, we could also assume lower initial values that have been enriched over time, suggesting degradation further upstream before arrival in the well (Table 2).

Table 2: Overview of CHCs found in the well fields, their potential origins and degradation processes based on the isotopic signatures from 2017 to 2020

The Houplin-Ancoisne and Seclin well fields were the least polluted in CHC. We found a mix of CHCs with low concentrations ranging from 0.2 (S1) to 8.8 µg L^{-1} (H7). Wells PZ51, H7, H4 and H1 were polluted mainly by PCE, TCE and TCA, while only TCE was detected in S1. The low CHCs concentrations can be explained by the minor presence of industrial activities in this area (Figure 1). Then, oxidizing conditions prevail in these well fields, the groundwaters provide conditions for aerobic biodegradation, except for H11 (dissolved oxygen <1 mg/L) where no CHCs were found (Figure 2-a). The absence of TCE- and PCE-degradation products such as *cis*-1,2-DCE suggested that reductive dechlorination does not occur, which is consistent with the observed groundwater geochemistry of these wells. 1,1-DCE could be a primary product from the plastics industry as in PZ56, or a product from previous dehydrochlorination of TCA.

4.3. Consequences for the further pumping operations

TCE, PCE and VC have regulation standards in the French legislation for their presence in drinking water (RF, 2007). In the studied well fields, the sum of TCE and PCE exceeds the threshold concentration of 10 µg L^{-1} in many wells (A12, A16, A18, A21, E5, E7, H7, PZ56, PZ59, and PZ61). VC exceeds the concentration limit (0.5 µg L^{-1}) in only two wells (A18 and PZ59) but is present and persistent in most wells. Our study showed that CHC degradation would be a long process in the well fields, even if this occurs in some part of the Chalk aquifer. In addition, the total amount of CHCs in

415 the surrounding soils probably can never been estimated, preventing a prediction of the time needed
416 for natural attenuation of this complex and diffuse—but also with hot spots—pollution. Currently,
417 drinking-water production uses dilution to reach the regulation CHC standards, but the lowering
418 water table makes this solution unsustainable. In order to continue producing drinking water from
419 the existing well fields, the operators need alternative solutions to reach the regulation CHC
420 standards.

421 The simplest solution would seem to be to adapt the pumping depth in the well. However, our study
422 of CHC concentrations in the PZ56 water column showed that TCE + PCE concentrations decrease
423 with depth, whereas VC shows an inverse trend (Table SI-3). Positioning of the pump is therefore
424 tricky and becomes impractical when the groundwater level lowers due to drought periods, as is
425 already frequently the case in this region. Then, an increase of the piezometric level leads to an
426 increase of CHC concentrations in the wells (for example, in the entire water column of PZ61 and in
427 shallower parts of PZ56 and PZ59 (Table SI-4)). The rise of the piezometric level induced by natural
428 recharge and decrease or stopping of pumping mobilize CHC sources present in surface. In order to
429 limit CHC contamination of the groundwater, as second option the water operators should adopt an
430 individual management of pumping wells in order to maintain the water table in the chalk and not in
431 the upper polluted layers. A third option is to create a protection front by discharging groundwater
432 from selected wells to protect the others from CHC plumes. These solutions require a sharp
433 identification in three dimensions of CHC fluxes in groundwater, but above all it involves wasting a
434 significant amount of water in a context of scarcity. A fourth solution would be to treat the water
435 with methods such as reverse osmosis, combinations of oxidants (e.g. ozone and UV), or
436 volatilization with a waterfall (Love Jr and Eilers, 1982; Foster et al., 1991). Overall, the better
437 understanding of the CHC behaviours described in this paper and the application of some of these
438 recommendations should undoubtedly ameliorate significantly the exploitation of this strategic
439 resource for the Lille Metropolis

5. Conclusions

Our study contributes to a better knowledge of CHC dynamics in a large strategic well field that supplies drinking water to the Lille European Metropolis. The distribution and concentrations of CHCs in the study area depends on two main factors. The first one is the past and current industrial activities in the area, causing broad CHC plumes in three dimensions that are further accentuated by pumping. The second one is the confined/unconfined nature of groundwater, causing reductive and/or oxidizing conditions that are favourable, or not, for efficient CHC degradation.

The strong *cis*-1,2-DCE pollution in the southwest of the Les Ansereuilles well field is due to the release of TCE—and its degradation by reductive dechlorination-from a former industrial laundry upstream of the studied wells. In the same well field, other wells are affected to a lesser extent by the release of PCE from several other industrial laundries, textile factories and dyeing industries, which again was partly degraded by reductive dechlorination. In the northern area of the well field, PCE, TCA, TCE and 1,1-DCE were found as primary products and *cis*-1,2-DCE as a degradation product of TCE by anaerobic biodegradation.

The other well fields (Houplin-Ancoisne, Seclin and Emmerin) are less impacted by CHC pollution, and no CHC degradation occurs in the wells as shown by the absence of degradation products, aerobic conditions, and isotopic signature of PCE.

The stratification of CHCs along the well-water columns, their steady concentrations over time caused by the large amount of available CHCs, and the little degradation occurring in the wells, all indicate that producing drinking water with a good quality from the well fields will be a major future challenge for water operators, as it is already. As observed in well PZ56, redox conditions and the degree of reductive dechlorination can vary over small distances, showing the importance of high-resolution sampling to demonstrate the attenuation of CHCs. Isotopic investigations combined with long-term monitoring of concentrations, taking into account spatial and in-depth heterogeneity, have proven to be an adequate methodology for identifying further CHC plumes and potential polluters

and demonstrating ongoing biodegradation activity within these plumes. The continuation of this monitoring strategy would also make it possible to control the efficiency of the remediation treatment that was recently undertaken.

6. Acknowledgements

This study was supported financially and technically by the Lille European Metropolis, the French Geological Survey (BRGM), the University of Lille, the Artois-Picardie Water Agency and the Haut-de-France Region in the context of projects COHMET (2017-2021), CLIMIBIO (2015-2020) and RESEAU (2016-2019). The authors thank Franck Joublin (BRGM), Paul Daudruy, Denis Poncin and Sébastien Knockaert (SOURCEO), Emmanuel Bugner, Jean-Noël Ottenwaelder and Isabelle Saunier (MEL laboratory) for their technical and scientific support during sampling and water analysis. We thank H.M. Kluijver for the English revision of the manuscript. The authors are grateful to the anonymous reviewer for thoughtful revision of the manuscript and constructive comments.

7. References

Aeppli, C., Berg, M., Cirpka, O.A., Holliger, C., Schwarzenbach, R.P., Hofstetter, T.B., 2009. Influence of mass-transfer limitations on carbon isotope fractionation during microbial dechlorination of trichloroethene. Environ. Sci. Technol. 43, 8813–8820.

Arcadis, 2016. Métropole Européenne de Lille, site des blanchisseries Tin - Don et Sainghin-en-Weppes (59). Diagnostic approfondi des sols, eaux souterraines et gaz du sol. Présentation des données. (No. AFR-DIA-10002-RPT-A01).

Arianna, A., Loris, C., Silvia, L., Valeria, M., Alessandra, P., Merri, A., Luca, A., 2019. Groundwater diffuse pollution in functional urban areas: The need to define anthropogenic diffuse pollution background levels. Sci. Total Environ. 656, 1207–1222.

Badin, A., Buttet, G., Maillard, J., Holliger, C., Hunkeler, D., 2014. Multiple dual C–Cl isotope patterns associated with reductive dechlorination of tetrachloroethene. Environ. Sci. Technol. 48, 9179–9186.

Bessière, H., Picot, J., Picot, G., Parmentier, M., 2015. Affinement du modèle hydrogéologique de la la Craie du Nord-Pas-de-Calais autour des champs captants de la métropole Lilloise. Rapport final.

Bloom, Y., Aravena, R., Hunkeler, D., Edwards, E., Frape, S.K., 2000. Carbon isotope fractionation during microbial dechlorination of trichloroethene, cis-1, 2-dichloroethene, and vinyl chloride: implications for assessment of natural attenuation. Environ. Sci. Technol. 34, 2768–2772.

Braeckevelt, M., Fischer, A., Kästner, M., 2012. Field applicability of Compound-Specific Isotope Analysis (CSIA) for characterization and quantification of in situ contaminant degradation in aquifers. Appl. Microbiol. Biotechnol. 94, 1401–1421.

Broholm, M.M., Hunkeler, D., Tuxen, N., Jeannottat, S., Scheutz, C., 2014. Stable carbon isotope analysis to distinguish biotic and abiotic degradation of 1, 1, 1-trichloroethane in groundwater sediments. Chemosphere 108, 265–273.

Cary, L., Benabderraziq, H., Elkhattabi, J., Gourcy, L., Parmentier, M., Picot, J., Khaska, M., Laurent, A., Négrel, P., 2014. Tracking selenium in the Chalk aquifer of northern France: Sr isotope constraints. Appl. Geochem. 48, 70–82.

Clement, T.P., Johnson, C.D., Sun, Y., Klecka, G.M., Bartlett, C., 2000. Natural attenuation of chlorinated ethene compounds: model development and field-scale application at the Dover site. J. Contam. Hydrol. 42, 113–140.

Clewell, H.J., Gentry, P.R., Gearhart, J.M., Allen, B.C., Andersen, M.E., 1995. Considering pharmacokinetic and mechanistic information in cancer risk assessments for environmental contaminants: examples with vinyl chloride and trichloroethylene. Chemosphere 31, 2561–2578.

Foster, D.M., Rachwal, A.J., White, S.L., 1991. New treatment processes for pesticides and chlorinated organics control in drinking water. Water Environ. J. 5, 466–476.

Giri, A.K., 1995. Genetic toxicology of vinyl chloride—a review. Mutat. Res. Genet. Toxicol. 339, 1–14.

Hunkeler, D., Aravena, R., Butler, B.J., 1999. Monitoring microbial dechlorination of tetrachloroethene (PCE) in groundwater using compound-specific stable carbon isotope ratios: Microcosm and field studies. Environ. Sci. Technol. 33, 2733–2738.

Hunkeler, D., Aravena, R., Cox, E., 2002. Carbon isotopes as a tool to evaluate the origin and fate of vinyl chloride: Laboratory experiments and modeling of isotope evolution. Environ. Sci. Technol. 36, 3378–3384.

Kawabe, Y., Komai, T., 2019. A case study of natural attenuation of chlorinated solvents under unstable groundwater conditions in Takahata, Japan. Bull. Environ. Contam. Toxicol. 102, 280–286.

La Vigna, F., Sbarbati, C., Bonfà, I., Martelli, S., Ticconi, L., Aleotti, L., Covarelli, A., Petitta, M., 2019. First survey on the occurrence of chlorinated solvents in groundwater of eastern sector of Rome. Rendiconti Lincei Sci. Fis. E Nat. 1–10.

Laaks, J., Jochmann, M.A., Schilling, B., Schmidt, T.C., 2010. In-tube extraction of volatile organic compounds from aqueous samples: an economical alternative to purge and trap enrichment. Anal. Chem. 82, 7641–7648.

Lee, C.C., Bhandari, J.C., Winston, J.M., House, W.B., Peters, P.J., Dixon, R.L., Woods, J.S., 1977. Inhalation toxicity of vinyl chloride and vinylidene chloride. Environ. Health Perspect. 21, 25–32.

Lee, P.K., Conrad, M.E., Alvarez-Cohen, L., 2007. Stable carbon isotope fractionation of chloroethenes by dehalorespiring isolates. Environ. Sci. Technol. 41, 4277–4285.

Lenczewski, M., Jardine, P., McKay, L., Layton, A., 2003. Natural attenuation of trichloroethylene in fractured shale bedrock. J. Contam. Hydrol. 64, 151–168.

Love Jr, O.T., Eilers, R.G., 1982. Treatment of drinking water containing trichloroethylene and related industrial solvents. J.-Am. Water Works Assoc. 74, 413–425.

Maréchal, J.-C., Dewandel, B., Subrahmanyam, K., 2004. Use of hydraulic tests at different scales to characterize fracture network properties in the weathered-fractured layer of a hard rock aquifer. Water Resour. Res. 40.

Maymó-Gatell, X., Nijenhuis, I., Zinder, S.H., 2001. Reductive dechlorination of cis-1, 2-dichloroethene and vinyl chloride by “Dehalococcoides ethenogenes.” Environ. Sci. Technol. 35, 516–521.

Palau, J., Marchesi, M., Chambon, J.C.C., Aravena, R., Canals, À., Binning, P.J., Bjerg, P.L., Otero, N., Soler, A., 2014. Multi-isotope (carbon and chlorine) analysis for fingerprinting and site characterization at a fractured bedrock aquifer contaminated by chlorinated ethenes. Sci. Total Environ. 475, 61–70. https://doi.org/10.1016/j.scitotenv.2013.12.059

Pooley, K.E., Blessing, M., Schmidt, T.C., Haderlein, S.B., MacQuarrie, K.T., Prommer, H., 2009. Aerobic biodegradation of chlorinated ethenes in a fractured bedrock aquifer: quantitative assessment by compound-specific isotope analysis (CSIA) and reactive transport modeling. Environ. Sci. Technol. 43, 7458–7464.

RF, 2007. Arrêté du 11 janvier 2007 relatif aux limites et références de qualité des eaux brutes et des eaux destinées à la consommation humaine mentionnées aux articles R. 1321-2, R. 1321-3, R. 1321-7 et R. 1321-38 du code de la santé publique.

Rivett, M.O., Lerner, D.N., Lloyd, J.W., 1990. Chlorinated solvents in UK aquifers. Water Environ. J. 4, 242–250.

Sherwood Lollar, B., Slater, G.F., Sleep, B., Witt, M., Klecka, G.M., Harkness, M., Spivack, J., 2001. Stable carbon isotope evidence for intrinsic bioremediation of tetrachloroethene and trichloroethene at area 6, Dover Air Force Base. Environ. Sci. Technol. 35, 261–269.

Sigg, L., 2000. Redox potential measurements in natural waters: significance, concepts and problems, in: Redox. Springer, pp. 1–12.

556 Slater, G.F., Sherwood Lollar, B., Sleep, B.E., Edwards, E.A., 2001. Variability in carbon isotopic fractionation
557 during biodegradation of chlorinated ethenes: implications for field applications. Environ. Sci. Technol.
558 35, 901–907.
559 van Warmerdam, E.M., Frape, S.K., Aravena, R., Drimmie, R.J., Flatt, H., Cherry, J.A., 1995. Stable chlorine and
560 carbon isotope measurements of selected chlorinated organic solvents. Appl. Geochem. 10, 547–552.
561 https://doi.org/10.1016/0883-2927(95)00025-9
562 Wanner, P., Hunkeler, D., 2015. Carbon and chlorine isotopologue fractionation of chlorinated hydrocarbons
563 during diffusion in water and low permeability sediments. Geochim. Cosmochim. Acta 157, 198–212.
564 https://doi.org/10.1016/j.gca.2015.02.034
565 Wiegert, C., Mandalakis, M., Knowles, T., Polymenakou, P.N., Aeppli, C., Macháčková, J., Holmstrand, H.,
566 Evershed, R.P., Pancost, R.D., Gustafsson, Ö., 2013. Carbon and chlorine isotope fractionation during
567 microbial degradation of tetra-and trichloroethene. Environ. Sci. Technol. 47, 6449–6456.
568 Witt, M.E., Klecka, G.M., Lutz, E.J., Ei, T.A., Grosso, N.R., Chapelle, F.H., 2002. Natural attenuation of chlorinated
569 solvents at Area 6, Dover Air Force Base: groundwater biogeochemistry. J. Contam. Hydrol. 57, 61–80.
570

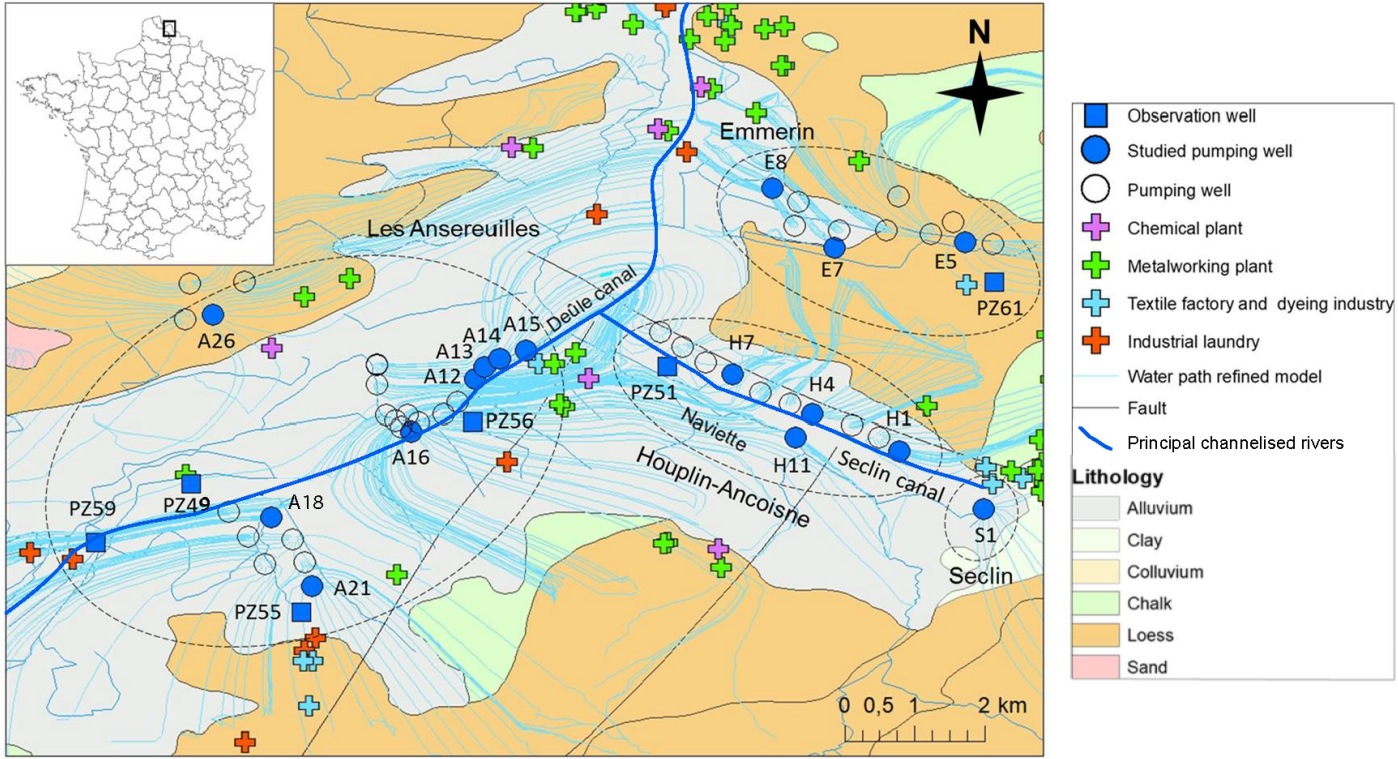
N
Emmerin
Les Ansereuilles
E8
E7
E5
PZ61
A26
A13
A14
A15
A12
Deûle canal
H7
PZ51
H4
H1
PZ56
A16
Naviette
H11
Seclin canal
Houplin-Ancoisne
PZ59
PZ49
A18
S1
Seclin
A21
PZ55
0 0,5 1 2 km
Observation well
Studied pumping well
Pumping well
Chemical plant
Metalworking plant
Textile factory and dyeing industry
Industrial laundry
Water path refined model
Fault
Principal channelised rivers
Lithology
Alluvium
Clay
Colluvium
Chalk
Loess
Sand

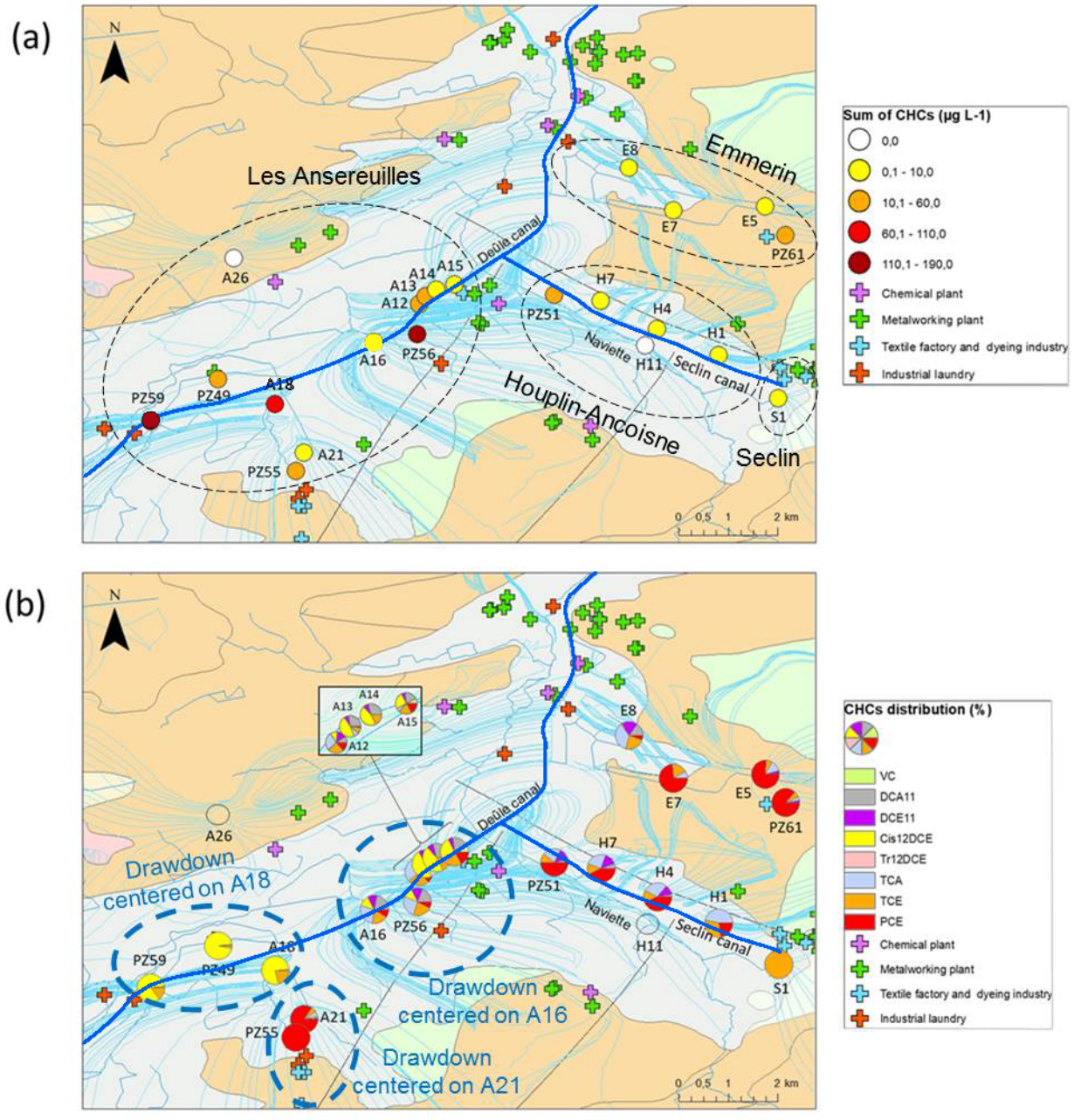
(a)
N
Les Ansereuilles
Emmerin
Houplin-Ancoisne
Seclin
Deûle canal
Naviette
Seclin canal
A26
A12
A13
A14
A15
A16
A18
A21
PZ49
PZ51
PZ55
PZ56
PZ59
PZ61
E5
E7
E8
H1
H4
H7
H11
S1
0 0,5 1 2 km
Sum of CHCs (µg L-1)
0,0
0,1 - 10,0
10,1 - 60,0
60,1 - 110,0
110,1 - 190,0
Chemical plant
Metalworking plant
Textile factory and dyeing industry
Industrial laundry
(b)
N
Drawdown centered on A18
Drawdown centered on A16
Drawdown centered on A21
CHCs distribution (%)
VC
DCA11
DCE11
Cis12DCE
Tr12DCE
TCA
TCE
PCE
Chemical plant
Metalworking plant
Textile factory and dyeing industry
Industrial laundry

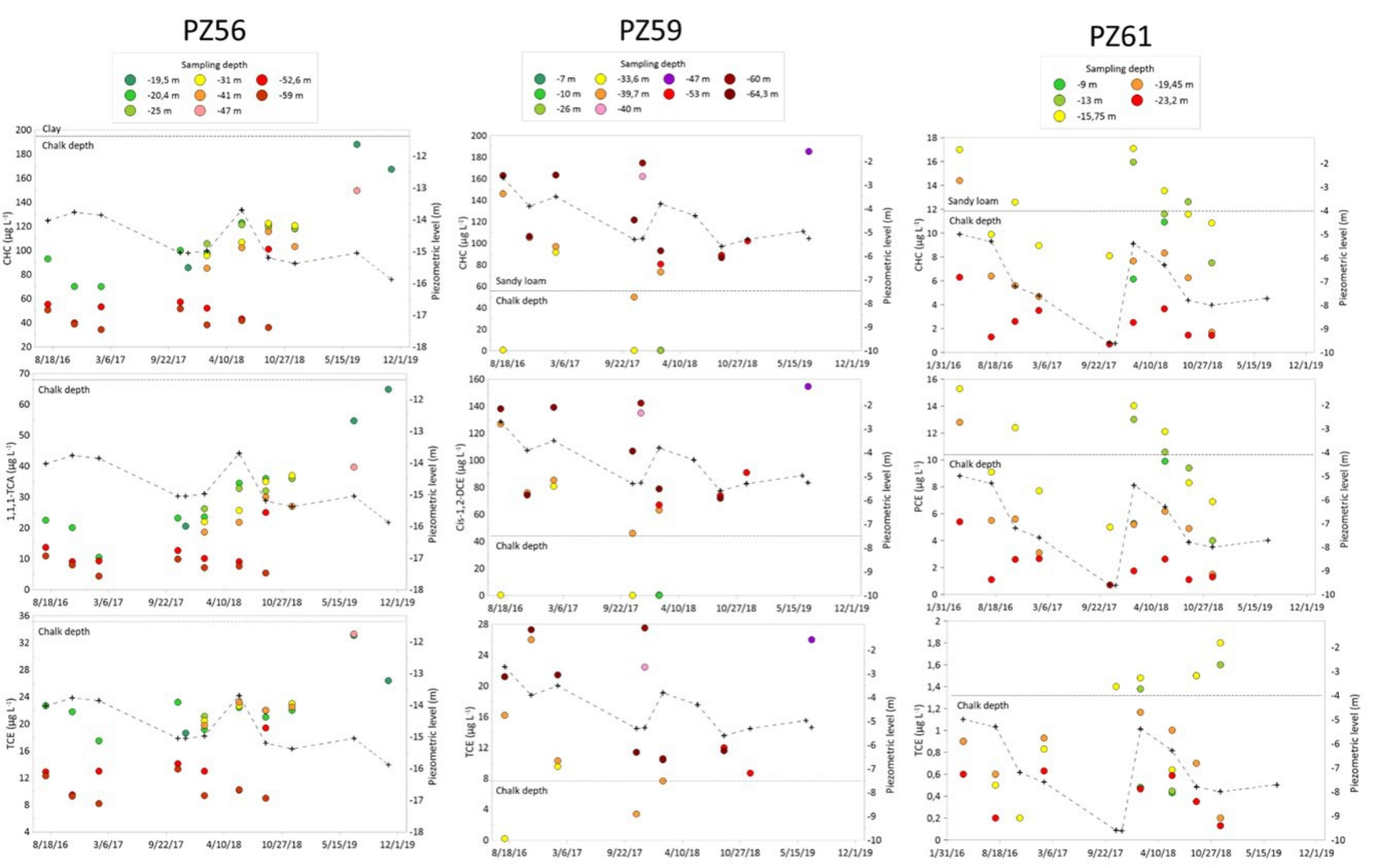
PZ56
PZ59
PZ61
Sampling depth
-19,5 m
-20,4 m
-25 m
-31 m
-41 m
-47 m
-52,6 m
-59 m
-7 m
-10 m
-26 m
-33,6 m
-39,7 m
-40 m
-47 m
-53 m
-60 m
-64,3 m
-9 m
-13 m
-15,75 m
-19,45 m
-23,2 m
Clay
Chalk depth
Sandy loam
CHC (µg L-1)
1,1,1-TCA (µg L-1)
Cis-1,2-DCE (µg L-1)
PCE (µg L-1)
TCE (µg L-1)
Piezometric level (m)
8/18/16
3/6/17
9/22/17
4/10/18
10/27/18
5/15/19
12/1/19
1/31/16

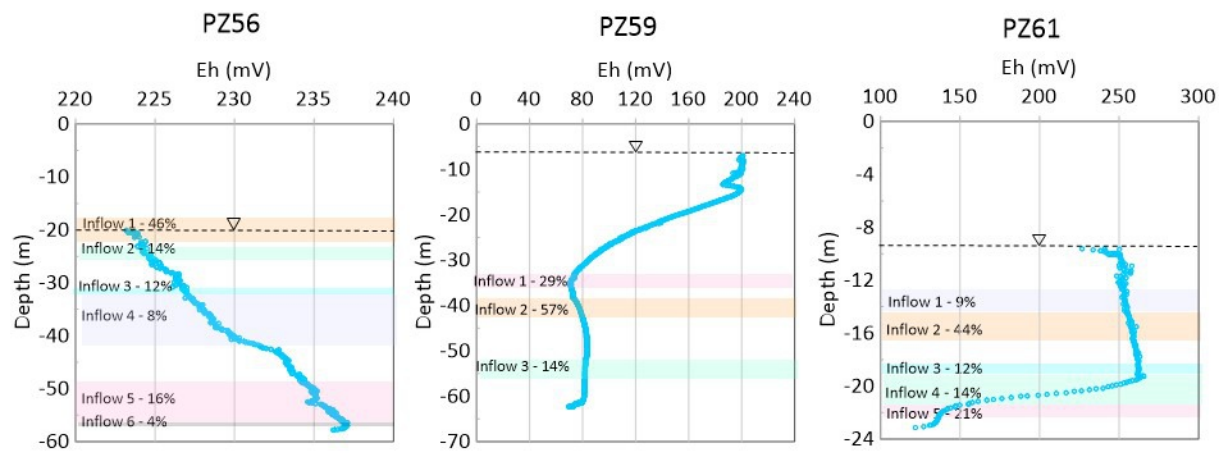
PZ56
Eh (mV)
220
225
230
235
240
0
-10
-20
-30
-40
-50
-60
Depth (m)
Inflow 1 - 46%
Inflow 2 - 14%
Inflow 3 - 12%
Inflow 4 - 8%
Inflow 5 - 16%
Inflow 6 - 4%
PZ59
Eh (mV)
0
40
80
120
160
200
240
0
-10
-20
-30
-40
-50
-60
-70
Depth (m)
Inflow 1 - 29%
Inflow 2 - 57%
Inflow 3 - 14%
PZ61
Eh (mV)
100
150
200
250
300
0
-4
-8
-12
-16
-20
-24
Depth (m)
Inflow 1 - 9%
Inflow 2 - 44%
Inflow 3 - 12%
Inflow 4 - 14%
Inflow 5 - 21%

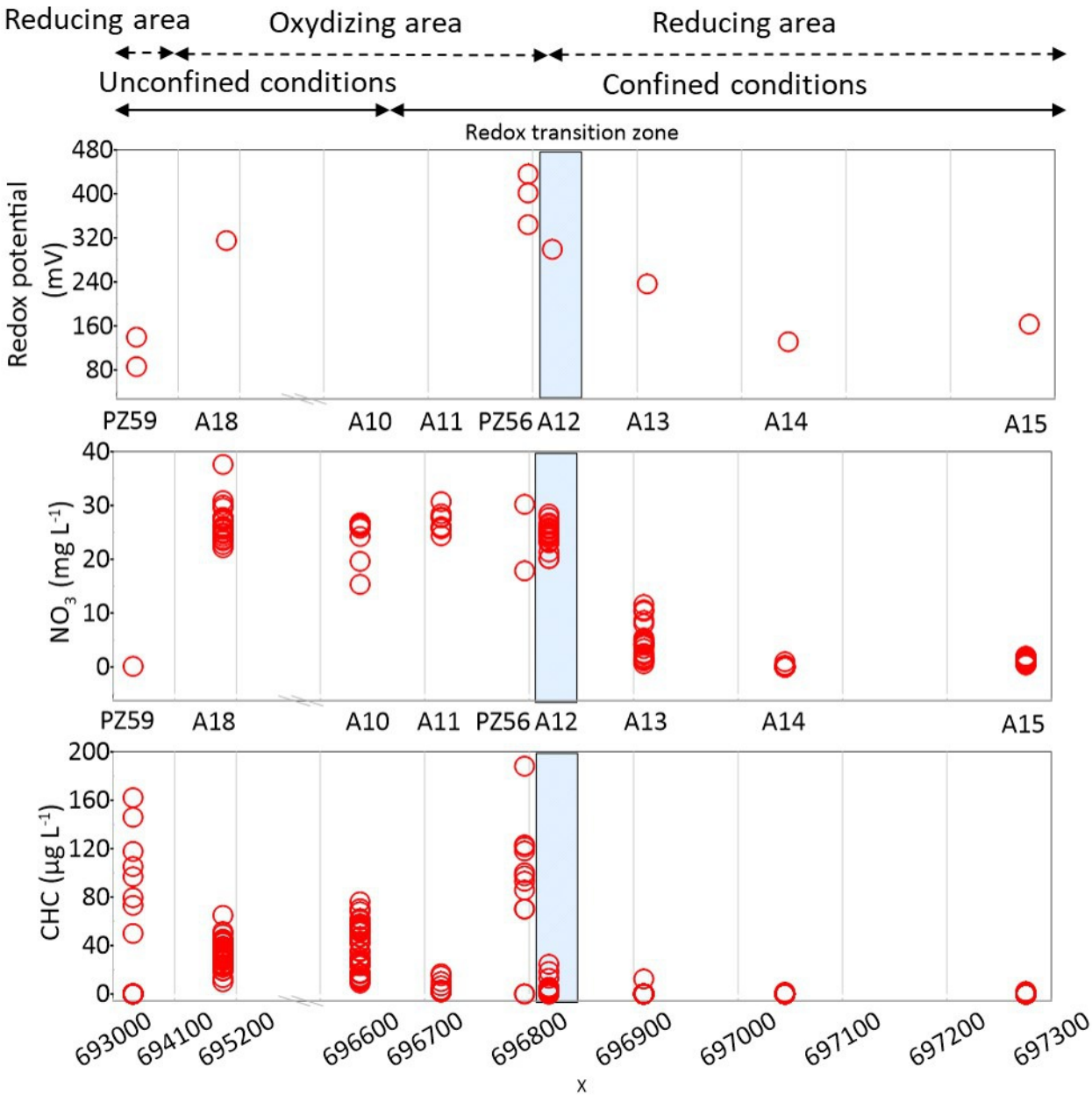
Reducing area
Oxydizing area
Reducing area
Unconfined conditions
Confined conditions
Redox transition zone
Redox potential (mV)
480
400
320
240
160
80
PZ59
A18
A10
A11
PZ56
A12
A13
A14
A15
NO3 (mg L-1)
40
30
20
10
0
CHC (µg L-1)
200
160
120
80
40
0
693000
694100
695200
696600
696700
696800
696900
697000
697100
697200
697300
X

Table 1: Stable carbon-isotope ratio $\delta^{13}C$ (in ‰ *vs* VPDB, ±0.5‰) and concentrations (µg L^{-1}) in the wells PZ49, PZ55, PZ56, PZ59 and PZ61 at several depths in 2017, 2019 and 2020.

Well	Depth (m)	Year of sampling		1,1-DCE	1,1-DCA	*Cis*-1,2-DCE	1,1,1-TCA	TCE	PCE
PZ49	-52	2017	$\delta^{13}C$ (‰)	-	-	-29.8	-	-	-
			Concentration (µg L^{-1})	-	-	18.5	-	-	-
	-47	2019	$\delta^{13}C$ (‰)	-	-	-29.7	-	-	-
			Concentration (µg L^{-1})	-	-	52.8	-	-	-
		2020	$\delta^{13}C$ (‰)	-	-	-29.6	-	-	-
			Concentration (µg L^{-1})	-	-	42.0	-	-	-
PZ55	-45	2017	$\delta^{13}C$ (‰)	-	-	-	-	-	-28.1
			Concentration (µg L^{-1})	-	-	-	-	-	29.0
	-31	2019	$\delta^{13}C$ (‰)	-	-	-	-	-	-25.9
			Concentration (µg L^{-1})	-	-	-	-	-	5.1
		2020	$\delta^{13}C$ (‰)	-	-	-	-	-	-26.5
			Concentration (µg L^{-1})	-	-	-	-	-	6.8
PZ56	-19,5	2017	$\delta^{13}C$ (‰)	-	-21.6	-22.9	-20.2	-20.5	-24.8
			Concentration (µg L^{-1})	-	15.2	12.8	21	18.6	7.3
		2019	$\delta^{13}C$ (‰)	-18.7	-22.1	-23.2	-21.3	-22.6	-24.9
			Concentration (µg L^{-1})	30.5	33.3	23.2	54.7	33.1	13.0
		2020	$\delta^{13}C$ (‰)	-	-	-	-	-19.4	-23.9
			Concentration (µg L^{-1})	-	-	-	-	17.1	6.5
	-47	2019	$\delta^{13}C$ (‰)	-17.5	-22.1	-23.1	-23.0	-20.5	-24.4
			Concentration (µg L^{-1})	19.9	27.8	17.4	39.7	33.3	11.2
		2020	$\delta^{13}C$ (‰)	-	-	-	-	-17.7	-
			Concentration (µg L^{-1})	-	-	-	-	10.4	-
PZ59	-40	2017	$\delta^{13}C$ (‰)	-	-	-31.8	-	-23.8	-
			Concentration (µg L^{-1})	-	-	135.0	-	22.0	-
		2019	$\delta^{13}C$ (‰)	-	-	-31.6	-	-24.2	-
			Concentration (µg L^{-1})	-	-	104.7	-	10.1	-
		2020	$\delta^{13}C$ (‰)	-	-	-31.8	-	-22.4	-
			Concentration (µg L^{-1})	-	-	102.0	-	8.6	-
	-47	2019	$\delta^{13}C$ (‰)	-	-	-31.8	-	-24.3	-
			Concentration (µg L^{-1})	-	-	154.7	-	25.9	-
	-60	2017	$\delta^{13}C$ (‰)	-	-	-31.7	-	-23.9	-
			Concentration (µg L^{-1})	-	-	142.0	-	28.0	-
		2020	$\delta^{13}C$ (‰)	-	-	-31.9	-	-23.0	-
			Concentration (µg L^{-1})	-	-	136	-	19.6	-
PZ61	-15	2017	$\delta^{13}C$ (‰)	-	-	-	-	-	-23.3
			Concentration (µg L^{-1})	-	-	-	-	-	8.9
		2019	$\delta^{13}C$ (‰)	-	-	-	-	-	-23.4
			Concentration (µg L^{-1})	-	-	-	-	-	13.6
		2020	$\delta^{13}C$ (‰)	-	-	-	-	-	-23.3
			Concentration (µg L^{-1})	-	-	-	-	-	12.2
A18	-41	2020	$\delta^{13}C$ (‰)	-	-	-	-	-	-
			Concentration (µg L^{-1})	-	-	3.6	0.9	-	-

Table 2: Overview of CHCs found in the well fields, their potential origins and degradation processes based on the isotopic signatures from 2017 to 2020

Well	CHC	Concentrations (µg L^{-1})	Potential origin	$\delta^{13}C$ (‰)	Suspected degradation process
PZ59	TCE	9-28	Upstream industrial laundry	-24.2 to -22.4	Reductive dechlorination (start in 2020) TCE → cDCE
	cDCE	102-155	Reductive dechlorination of TCE	-31.9 to -31.6	Reductive dechlorination (limited, accumulation of cDCE) cDCE→VC→CH_4
PZ49	cDCE	19-42	PZ59 ? Reductive dechlorination of TCE	-29.8 to -29.6	No further degradation
PZ55	PCE	5-29	Upstream industrial sites?	-28.1 to -25.9	Reductive dechlorination PCE →cDCE
PZ56	1,1-DCE	20-31	From additional source or reductive dechlorination of cDCE or dehydrochlorination of TCA	-18.7 to -17.5	No process evidenced
	1,1-DCA	15-33	Reductive dechlorination of TCA	-22.6 to -22.1	No process evidenced
	cDCE	13-23	Reductive dechlorination of TCE	-23.1 to -22.9	Reductive dechlorination? cDCE → 1,1-DCE
	TCA	21-55	No potential source identified	-23.0 to -20.2	Reductive dechlorination TCA → 1,1-DCA
	TCE	17-33	From additional source or reductive dechlorination of PCE	-22.6 to -20.5	Reductive dechlorination TCE → cDCE
	PCE	7-13	No potential source identified	-24.9 to -24.4	Reductive dechlorination PCE → TCE
PZ61	PCE	9-14	No source identified	-23.4 to -23.3	No degradation

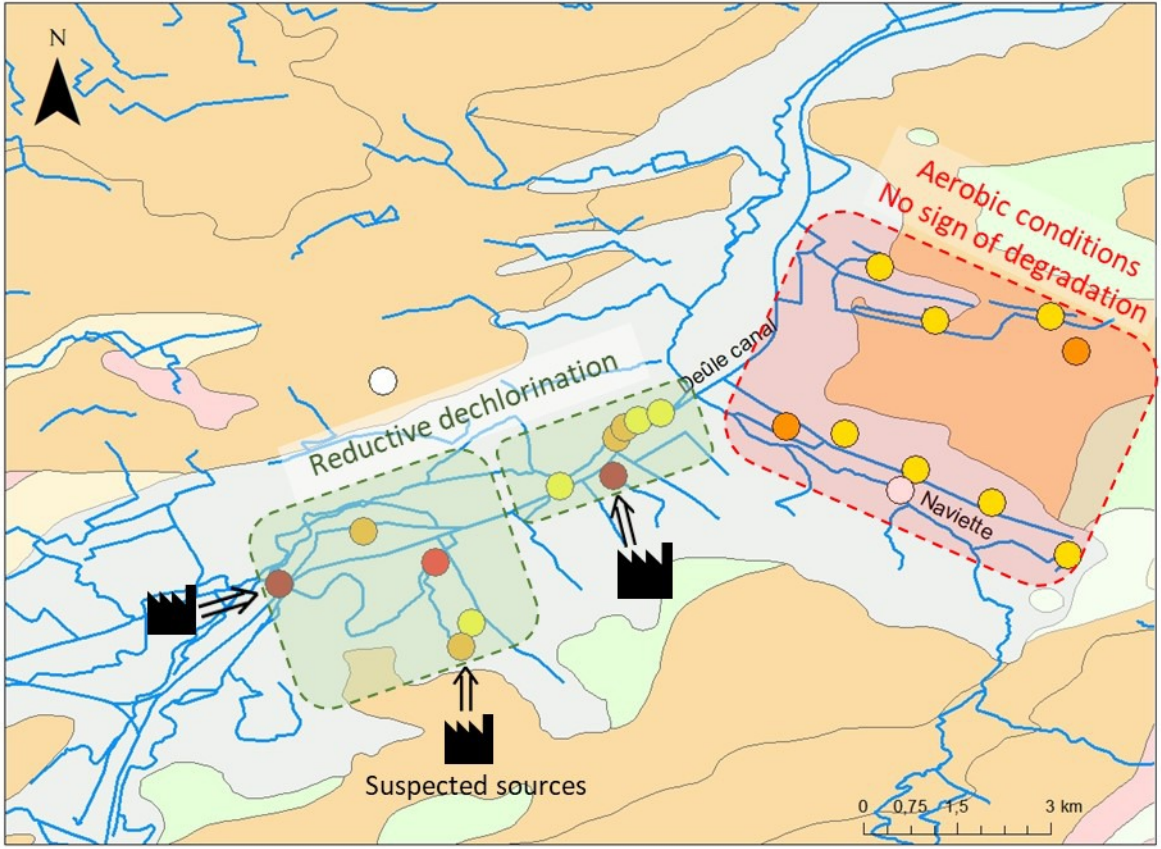
N
Aerobic conditions
No sign of degradation
Reductive dechlorination
Deûle canal
Naviette
Suspected sources
0 0,75 1,5 3 km